Evaluation and microanalytical study of ZVI /zeolite substrate mixtures for treating acid mine drainage using reactive barriers - removal mechanisms

D. Limper, G.P Fellinger, S.O Ekolu

University of Johannesburg, PO Box 524, Auckland Park 2006, South Africa.

Abstract

Batch and column experiments were performed to evaluate contaminant removal from acid mine drainage (AMD) using volcanic ash zeolite (VA) with or without zero-valent iron (ZVI) media. Two types of AMD were used i.e. WZ with pH of 2.43 taken from goldfields and TDB with pH of 2.93 collected from coalfields. It was found that VA substrate performed similarly or better than ZVI reactive media whose pH reached 7.0 to 8.5. VA was effective in removing heavy metals despite attaining a relatively lower maximum pH of 5.5. Metals Al, Fe, Zn were generally completely removed from both types of AMD by both the VA and ZVI substrates and their 50:50 mixtures. Removal of Mg and Mn was influenced by the type of AMD. Generally, the substrate comprising 50:50 ZVI/VA mixture was found to treat both AMD types fairly consistently, achieving complete removal of major elements in TDB and a majority of other elements in WZ.

Hematite and Goethite minerals were formed when ZVI was used to treat AMD while use of VA led to enhancement of Diopside and Augite along with formation of new phases Forsterite and Ferroan. Geochemical changes and microanalytical investigations altogether indicate pH-dependant chemical precipitation to be the main mechanism of heavy metal removal by ZVI, while adsorption and cation exchange processes were found to be responsible for pollutant removal by VA.

Keywords: Zero-valent iron; volcanic ash zeolite; permeable reactive barriers; acid mine drainage; heavy metals removal; batch and column tests

1. Introduction

Permeable reactive barriers (PRBs) are a promising alternative system for passive groundwater remediation. In most cases, PRBs are considered to be more cost effective relative to active treatment systems, as they require no operational cost and incur minimal maintenance (Obiri-Nyarko et al. 2014; Thiruvenkatachari et al. 2008; Morrison et al. 2003; Gavaskar 1999; Gavaskar et al. 1998; Waite et al. 2003; Day et al. 1999; Mulligan et al. 2001; Ekolu et al. 2014; 2016; Shabalala et al. 2017). While PRB systems are already established, this technology continues to develop as new and innovative reactive materials are sought to treat different types of contaminants. Industrial exploits of humankind have led to release of various kinds of toxic heavy metals into the environment including formation of acid mine drainage (AMD), leading to adverse soil and water pollution problems, related to accumulation of common elements such as Al^{3+}, Cr^{3+}, Ce^{3+}, Fe^{3+}, K^{+}, Mg^{2+}, Mn^{2+}, Na, and Zn^{2+}.

While several treatment processes including ion exchange, precipitation, phytoextraction, ultrafiltration, reverse osmosis, and electrodialysis (Harrison 2007; Fu and Wang 2011; Hashim et al. 2011) may be applied to remediate polluted water, the use of alternative low-cost materials as reactive media for contaminant removal by PRBs, is of great interest. Zero-Valent Iron (ZVI) is considered to be a conventional, reactive medium which has been widely used in PRB systems for contaminant removal from aqueous systems (Cundy et al. 2008; Bartzas et al. 2006; Komnitsas 2009; Johnson et al. 1996, 2003; Klimkova et al. 2011; Lien et al. 2005). However, when ZVI is used on its own, severe permeability problems are bound to

occur, causing clogging and reducing the barrier's hydraulic performance. Studies have shown that low-cost adsorbents such as naturally occurring zeolites could be used with or without ZVI (Delkash et al. 2015; Inglezakis 2005; Bosco et al. 2005).

There are numerous materials that could potentially be used as PRB reactive media for remediating acidic groundwater. However, before these materials may be selected, various factors need to be considered. A suitable PRB should contain reactive materials that have various characteristics (Xenidis et al. 2002) comprising: The ability to increase pH of the acidic groundwater, suitable porosity that allows groundwater to flow freely, acceptable lifespan, environmental compatibility, cost effectiveness and availability in large amounts, safe for handling and health of workers.

One of the important problems regarding use of ZVI as reactive media is the reduction of its hydraulic conductivity over time, due to oxidation of ZVI and formation of corrosion products such as metal precipitates, which in turn cause clogging of pores within the barrier system. To mitigate this problem, ZVI is often mixed with a passive medium such as sand which helps to reduce clogging and in turn extend lifespan of the PRB, but this measure also reduces treatment efficiency. There are continued research efforts towards developing more efficient or effective reactive media for optimum contaminant removal, prolonged permeability and cost effectiveness as indicated by various literatures. Attempts have been made to use zeolites for this purpose, in forms of pumice or volcanic ash as partial replacement for ZVI. Replacement levels of 50 to 70% pumice are reported to be optimal in media reactivity, hydraulic performance and cost effectiveness (Calabrò et al. 2012; Moraci and Calabrò, 2010).

The present study focussed on microanalytical characterisation and removal mechanisms of substrates containing VA, based on batch and column experiments conducted using naturally occurring AMD taken from a gold mine (WZ) and from a coal mine (TDB).

Measurements included pH and geochemical changes, adsorption and mass balance calculations. Analytical studies were done using x-ray diffraction (XRD), scanning electron microscopy (SEM) and Fourier transform infrared spectroscopy (FTIR) techniques.

2. Literature review

2.1 Zero-valent iron and clogging of reactive barriers

ZVI is elemental metallic iron that carries a zero charge on each atom, due to filling of its outer shell valency. ZVI is commonly used as a reactive medium in PRBs, owing to its ability to degrade organic substances and decompose some inorganic compounds (Xenidis et al. 2002; Klimkova et al. 2011; Lien et al. 2005). Processes such as redox reactions, precipitation, adsorption, ion exchange and biodegradation are responsible for decomposition and degradation of these compounds (Simon and Meggyes 2000). The ZVI for use as reactive media in PRB's, should have a high iron content, low carbon content and non-toxic metals. The particle sizes of ZVI used in PRBs typically range between 0.25 - 2.0 mm diameters, to ensure permissible hydraulic conductivity and effective surface area usually between 0.5 - 1.5 m^2/g respectively (Bilardi 2011). Use of fine-grained ZVI particles smaller than 1.0 mm diameter in PRBs, increases reaction rates due to higher surface area (Ruhl and Jekel, 2012). However, these fine particles may severely reduce hydraulic conductivity of reactive barriers, leading to a relatively short lifespan due to clogging arising from porosity losses. Clogging results from formation of $Fe(OH)_2$ precipitates in the short-term. In the long term, $Fe(OH)_2$ and $FeCO_3$ precipitates tend to form in low carbonate water, while $Fe(OH)_2$, $FeCO_3$ and CaCO3 may form in high carbonate water (Mackenzie et al. 1999). Anaerobic iron corrosion may also be significantly enhanced by carbonate levels in water, which in turn impacts both ZVI reactivity and hydraulic conductivity (Weber et al. 2013). The Kozeny–Carman equation (Jeen et al., 2011) may be applied to account for the impact of porosity losses on hydraulic

conductivity of a reactive barrier. Only few researches have attempted to mitigate hydraulic conductivity loss by employing combinations of reactive materials including blending of ZVI with other kinds of reactive materials especially pumice (Bilardi 2011; Obiri-Nyarko et al. 2014; Moraci N. 2010).

2.2 Use of zeolite for removal of contaminants from polluted water

Volcanic scoria pumice or ash (VA) is a naturally occurring aluminosilicate mineral, belonging to the class of "tectosilicate" minerals. The structures of zeolites consist of three dimensional frameworks of SiO_4 and AlO_4 tetrahedra. Aluminium ion is small enough to occupy a position at centre of the tetrahedron of four oxygen atoms, while the isomorphous replacement of Si^{4+} by Al^{3+} produces a negative charge in the lattice. The net negative charge is balanced by an exchangeable cation (Al^{3+}, Cr^{3+}, Ce^{3+}, Fe^{3+}, K^{+}, Mg^{2+}, Mn^{2+}, Na and Zn^{2+}) that is present in AMD. The fact that zeolite exchangeable ions are relatively harmless makes them particularly suitable for removing undesirable heavy metal ions from AMD (Pitcher et al., 2004; Cyrus and Reddy, 2011; Delkash et al. 2015; Erdem et al. 2004; Inglezakis 2005; Li et al. 2015).

Various researches (Wan et al., 2017; Abdel Salam et al., 2011; Díaz, 2017; Rios et al., 2008; Wajima, 2013), have indicated cation exchange and adsorbent mechanisms as the main processes for effectiveness of zeolites in pollutant removal from contaminated water. Ion exchange occurs when free ions in zeolite diffuse into solution while ions in water diffusion into the zeolite molecular structure (Inglezakis, 2005). Zeolite typically exhibit predominant intake of cations in polluted water with limited release of its own free ions into solution, a processes which characterises its adsorbent properties. Zeolites have been widely studied for removal of heavy metals from polluted water such as wastewater (Toscano et al., 2008; Abdel Salam et al., 2011), acid mine drainage (Motsi et al., 2009; Nekhunguni et al.,

2017; Itskos et al., 2015; Abdel Rahmana et al. 2012) and contaminated soils (Querol et al., 2006). Basaldella et al (2007) reported co-existence of all three mechanisms of adsorption, cation exchanged and chemical precipitation. They found that increase in solution pH promoted the precipitation mechanism and led to higher removal capacity of chromium pollutant by zeolite. Field based zeolite PRB installations have also been studied in relation to media reactivity and hydraulic performance (Fuhrmann et al., 1995; Mumford et al., 2013; 2014), the latter being determined as the more crucial parameter than the former.

3. Materials and Methods

3.1 Reactive media

The reactive materials used in batch and column tests consisted of ZVI or Fe^0 and VA. Two sizes of steel grit, supplied by B.V Products SA (pty) Ltd GH 18 of 1.0 - 1.4 mm diameter particles and GH 80 of 0.18 - 0.425 mm diameter, were blended in equal proportions and used in the investigation. Its chemical composition was 80.6% Fe_2O_3, 0.72% MnO, 0.24% Al_2O_3, 0.19% Cr_2O_3, 0.03% MgO, 0.02%ZnO and trace elements. The VA used was obtained from its natural origins at the Rwenzori mountain range, an upfault of the Western Rift Valley in East Africa (Ekolu et al. 2006). The chemical composition of VA was 42.8% SiO_2, 14.6% Al_2O_3, 13.5% Fe_2O_3, 10% CaO, 6.95% MgO, 0.22% SO_3, 3.21% K_2O, 3.3% Na_2O, 3.48% TiO_2, 0.22% MnO. VA particle sizes of 1.18 to 2.00 mm diameter were prepared for use in the experiments.

3.2 Acid mine drainage

AMD was obtained from two sources comprising an abandoned open cast coal mine, designated as TDB, and a gold mine decanting underground water from deep shafts, WZ. The two AMD types had different chemical compositions. The pH values of WZ and TDB were

2.46 and 2.93 respectively. Table 1 shows element concentrations in the raw AMD used in this study.

Table 1. Composition of acid mine drainage

AMD type	Element concentration (mg/l)										
	Al	Ce	Cr	Fe	K	Mg	Mn	Na	Zn	SO_4	PO_4
WZ	2.30	0.05	0.002	7.91	8.39	131.35	88.92	104.09	0.54	1123	0.83
TDB	6.11	0.006	0.002	7.27	38.48	171.05	12.72	2496.7	1.02	2870	0.77

3.3 Batch and column tests

ZVI and VA were prepared in various proportions of 100ZVI, 100VA, 50:50ZVI-VA, 70:30ZVI-VA. Table 2 gives the quantities of reactive materials employed in preparing the various mixtures. Batch tests are typically used as a screening method for evaluating and selecting suitable substrates for treatment of AMD. In this study, trial batch tests were conducted for 14 days. A second batch test was also conducted to replicate results of trial batches.

Batch experiments were performed by mixing the reactive media with WZ and TDB in plastic containers i.e reactors. Test samples of treated AMD were removed from reactors every 24 hours and placed in plastic vials. The samples were immediately tested for pH upon their removal from reactor batch containers, and then stored for water analysis which was done using Inductively Coupled Plasma Optical Emission Spectrometry (ICP-OES). The pH meter used, MP-103 microprocessor-based pH/mV/Temp tester, was calibrated after every twentieth reading according to the manufacturer's specifications (Shabalala et al. 2017). After

each calibration, the pH test meter provided a digital display of the instruments reading accuracy, which ranged between 96% and 93%.

Column tests are typically used to determine the design parameters for PRBs under dynamic AMD flow conditions. These parameters include half-life estimation and non-linear sorption of elements to non-reactive sites (Motsi et al. 2009). Since concentrations of pollutants and inorganic elements change with distance as AMD flows through the reactive cell, these changes can be monitored by fitting sampling ports along column length.

Table 2. ZVI-VA mixtures used for batch and column tests

Sample No		100 ZVI	100VA	50:50ZVI-VA	70:30ZVI-VA
Description		100% ZVI	100%VA	50%ZVI+50% VA	70%ZVI +30%VA
Mass of ZVI (g)	GH 18	2 197	0	1 099	1 538
	GH 80	1 670	0	835	1 169
Mass of VA (g)		0	1 028	514	308
Volume of AMD (L)		2	2	2	2

Six columns 650 mm in height were made from polyvinyl chloride (PVC) pipes. Each column had four sampling ports that were distributed along its length at 150 mm spacing intervals. The lower three sampling ports were used for taking out treated AMD samples while the outflow effluent was collected from the fourth, upper port. Three columns were used for each of the AMD types, WZ and TDB. Figure 1 shows the setup of columns during the progress of testing. AMD was continuously pumped from reservoirs containing WZ and TDB through the reactor bed within the columns. Submersible pumps of 1.2 m constant head were used to pump raw AMD through the columns, at a slow flow rate of 0.1 mls per minute.

Samples were collected from ports every 24 hours over a period of 42 days of the experiment. Water analysis of the samples was done using ICP-OES.

3.4 Preparation of liquid and solid samples

3.4.1 Water samples

Test samples of treated AMD that were collected from batch and column tests, were first filtered to remove solids greater than 0.45 µm. This was done by using a 20 mL medical grade syringe, 0.45 µm syringe filter and a multichannel electronic pipette. An exact amount of 9.9 mL of filtered sample was added to the centrifuge tube containing 0.1 mL of HNO_3, in order to dissolve the sample. To avoid cross-contamination, none of the filters, syringes or pipette tips were re-used. After filtration and dissolution was complete, the vials were marked and filled with samples, capped and placed on a vortex mixer to ensure thorough mixing. Finally, the vials were placed in an autosample holder and stored at 4^{o}C until testing.

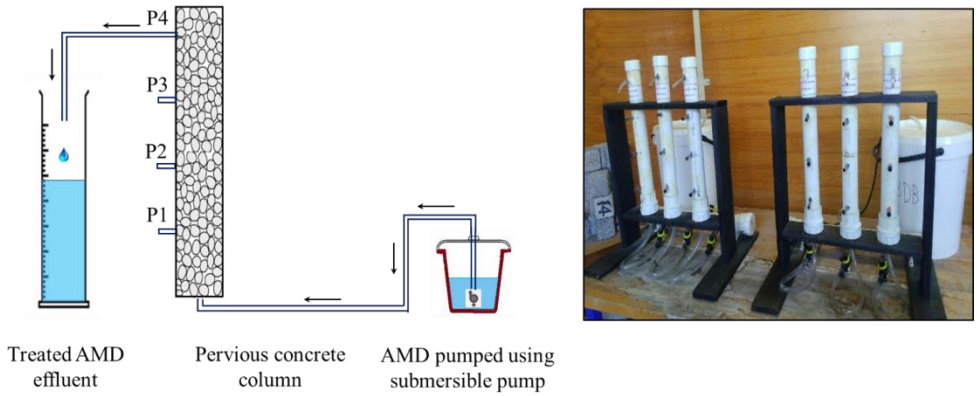

(Adapted from Shabalala et al. 2017)

Figure 1. Set up of the column test experiment

3.4.2 Digestion of solid residues

Solid residues of ZVI or VA before and after reaction with AMD, were also chemically analysed. The first step was digestion involving weighing out 1g of solid sample using an

analytical laboratory scale. Once all the samples had been weighed, the solid samples were placed in Teflon microwave tubes. The digestion process was initiated once 9 mls of HCl and 3 mls HNO_3 were introduced. The digestion tubes were capped and placed in a carousel that was then inserted into the CEM Mars 6 microwave digester heated at 500 Watts to a maximum temperature of 2000^{o}C. Digestion was conducted for 40 mins. After the digestion was complete, samples were prepared for chemical analysis as described in Section 3.4.1. Dilution of samples was done by adding 10 mL of the digested sample to 40 mL of deionized water in a volumetric flask. These were mixed and then added to the centrifuge tubes.

3.5 Mineralogical and microscopic examination of solid residues

XRD studies and microscopic analyses were conducted on substrates before and after their exposure to AMD. These samples of substrates were oven-dried at 40^{o}C for 24 hours, to remove moisture that could interfere with analysis. VA substrates were ground to fine powder and pressed into sample holders. Because of difficulty in grinding ZVI, the finest particles where sieved and used in the analyses.

XRD analysis was conducted using X-ray diffractometer model X'pert PRO PW3830. Holders containing powder samples where placed on a sample tray then inserted into the instrument, and left to run overnight; results were obtained the following day. The electron microscope TESCAN VEGA3SEM coupled with AZtec energy dispersive spectroscopy (EDS) was used for SEM analysis. Representative samples for microscopic examination, prepared as explained in the foregoing, were stuck onto the aluminium mounting stubs using a double-sided carbon tape used to aid conductivity of the sample. Carbon coating was then done to ensure that non-conducive elements in the sample could be analysed or detected by SEM. In analysing each sample, representative SEM images were captured. Using the backscattered electron (BSE) detector, inspection of the image was done to locate possible

sites where crystalline or other major phases had formed. Upon detection of such a site, an image was generated through secondary electron (SE) and BSE modes. Close inspection was done and more micrographs were generated. Spot elemental analysis and/or mapping were also done using EDS to determine the different types of elements present and/or the possible crystalline structures that formed during treatment of AMD.

4. Results and discussions

4.1 Batch test results

4.1.1 pH measurements

All the batch experiments that were conducted exhibited rapid increase in pH during the first 4 to 5 days. TDB showed more rapid rise in pH than WZ. In batches containing ZVI or ZVI/VA blends, WZ consistently yielded lower peak measurement of about pH = 7 to 7.5, compared to pH = 8.0 to 8.7 for TDB, as shown in Figure 2. Accordingly, TDB gave pH values that were about one unit higher than the values obtained for WZ. The different responses of these two AMD types may be attributed to their different chemical compositions. Evidently, TDB had relatively higher content of alkalis, about 5 to 25 times higher than in WZ. Na and K concentrations were respectively 2496.7 mg/l and 38.5 mg/l in TDB compared to much lower levels of 104.1 mg/l and 8.4 mg/l in WZ (Table 1). In the same vein, raw WZ had a lower initial pH of 2.46 compared to pH of 2.93 for TDB. Since OH^- ions from ZVI corrosion add to the existing alkalis in the AMD, it can be expected that TDB had a much higher release of OH^- during its treatment, relative to WZ. However, there is a possibility of more complex interactions among various ions, which could variously affect treatability of the different AMD types.

The 100VA substrate exhibited more rapid pH increase, reaching peak pH values within two days, compared to 4 or 5 days for 100 ZVI. Despite its rapid increase in pH, the

maximum value obtained for 100VA reactive material was only pH = 5.5, which is considerably lower than pH values for batch mixtures containing ZVI. However, it can be seen in Figure 2 that 100VA gives similar peak pH values for both WZ and TDB, unlike mixtures containing ZVI for which TDB had higher peak pH values than WZ.

4.1.2 Removal of contaminants

Figure 3 shows changes in concentration of contaminants during the batch test. Results are shown for both TDB and WZ treated, using the reactive materials 100ZVI, 100VA, and mixture 50:50ZVI-VA. Graphs in Figure 3(a1) to (a5) provide results for AMD that was treated using 100ZVI or 100VA while graphs in Figure 3(b1) to (b5) give results obtained when the mixture 50:50ZVI-VA was used. It is interesting to note that despite the low pH of 5.5 attained by VA (Figure 2), its effectiveness in removing contaminants is similar or better than that of ZVI which had higher pH = 7 to 8.7 depending on the type of AMD. VA showed more rapid removal of some contaminants such as Fe, relative to the action by 100ZVI or 50:50ZVI-VA.

Evidently, all the reactive materials used in the batch tests, did effectively remove Al, Fe and Zn within the first three days of treatment. It is notable in Figure 3(a2) that there was rapid increase in Fe concentration from day 1 to 3 for the batch tests containing ZVI, which may be attributed to initial dissolution of iron from ZVI by the acidic AMD, prior to its hydrolysis leading to later rise in pH. In graphs of Figure 3(a3) and (b3), it is evident that Mg concentration in the WZ remained unchanged in all the reactive media used, as the pH in WZ remained below 7.5. However, Mg concentration in TDB initially remained unchanged until after day 3 when it began to precipitate and later was completely removed from the AMD. It is known that Mg does not precipitate until pH exceeds 9. In the ZVI batch tests for TDB, the pH surpassed 8.3 on day 3, triggering precipitation of Mg from this AMD. Interestingly, it

appears the zeolite 100VA released some Mg into solution during the first three days causing its increase, which was followed by its removal at later ages despite the low pH = 5.5. The reason for this complex behaviour is not clear but may be related to the cation exchange mechanism of VA. Mn is generally removed at pH = 9 to 9.5 which was not attained by any of the reactive materials or their combinations. Indeed, it can be clearly seen in Figures 3a(4) and 3b(4), that the Mn concentration in TDB remained unchanged at pH values of up to 8.7. However, the WZ which had lower pH = 7.0 to 7.5 showed some gradual decrease in Mn concentration. This reduction is certainly not related to pH but may be associated with co-precipitation perhaps with Fe, considering that at day 1 to 3, WZ had higher Fe concentration than TDB.

The alkalis, Na and K are highly mobile ions which are not pH dependent bases. Accordingly, their concentrations in treated AMD are not expected to follow similar trends as metal precipitation. It was observed that the concentration of K in ZVI-treated AMD, remained unchanged throughout the duration of the test. The reactive materials containing VA zeolite, released some Na and K into solution leading to elevation of their concentrations at early ages but the elements were subsequently removed. The geochemical composition of AMD evidently played a key role, as observed with Na and K of TDB which were readily removed while those in WZ remained generally unchanged.

The VA also released Zn into solution causing its elevated concentration in both the WZ and TDB as seen in Figure 3(a5). This Zn release from VA at early stages, in turn had the effect of delaying Zn removal from AMD but the behaviour was avoided in 50:50ZVI-VA. Compared to 100ZVI and 100VA, contaminant removal by 50:50ZVI-VA was similar or better. These findings are consistent with those reported by Calabrò et al. (2012) who concluded that replacement of ZVI by 50% pumice provided the most efficient performance to remove Ni from polluted solutions, relative to replacements of 70 or 90% pumice.

In the present investigation, contaminant removal efficiency was determined for major elements, by calculating the proportion of metal ions removed using the expression:

$$\text{Removal efficiency}\,(\%) = \frac{C_o - C_f}{C_o}\, x\, 100$$

Where C_o and C_f are the initial and final concentrations of a given contaminant in the AMD solution. Table 3 gives the removal levels of various elements for the 100ZVI, 100VA, and 50:50 ZVI/VA reactive media. It is clear that all the media are effective in complete removal of Al, Fe and Zn. Again, it is evident that for TDB, complete removal of the major elements was achieved by 100VA or 50:50 ZVI/VA while 100ZVI was not effective in removing potassium. For WZ, neither of the reactive media were able to remove K or Na alkalis. Clearly, the geochemical composition of the two AMD types was a key factor, as mentioned earlier.

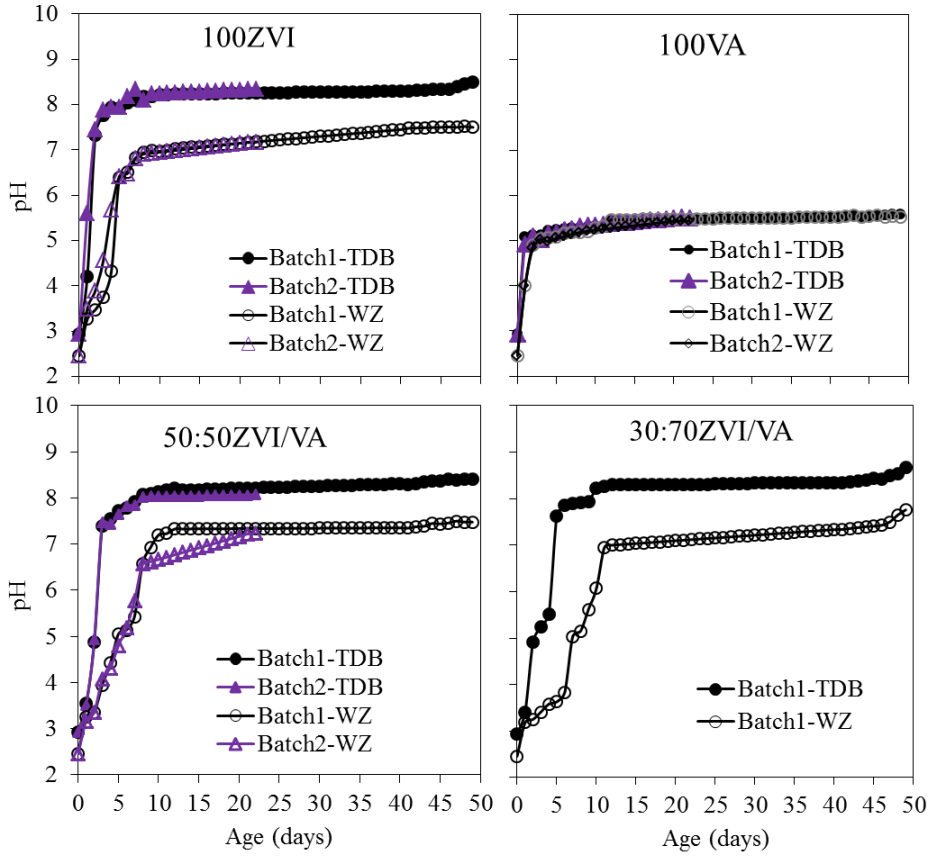

Figure 2. pH measurements for batch mixtures

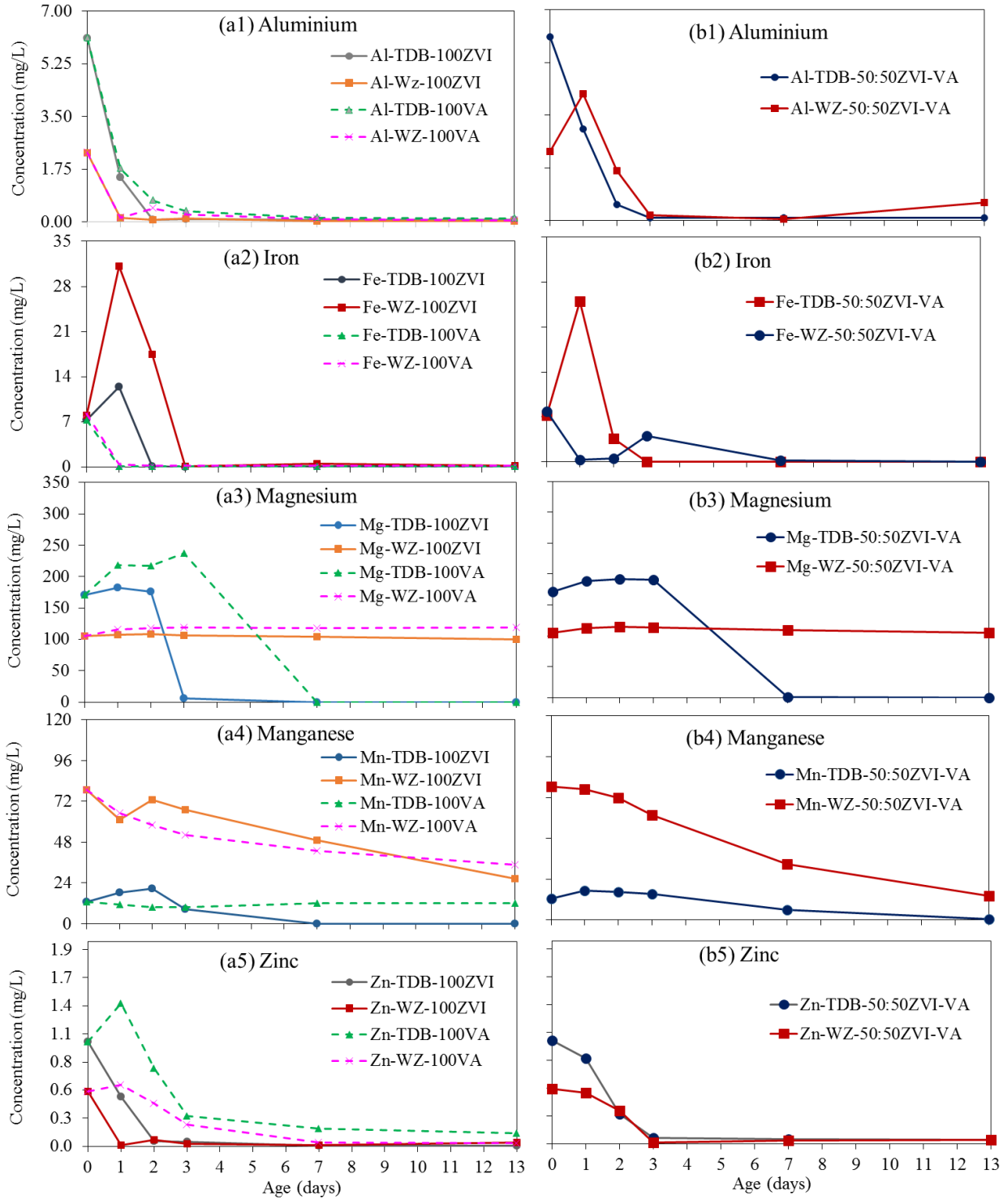

Figure 3. Changes in element concentrations during batch tests

Table 3. Contaminant removal efficiency levels for volcanic ash zeolite and ZVI reactive media

AMD Type	Reactive Media	Al (%)	Fe (%)	K (%)	Mg (%)	Mn (%)	Na (%)	Zn (%)
TDB	100VA	98.2	99.7	99.9	100	6.1	99.8	87.4
	100ZVI	98.9	99.9	-5.6	100	99.9	99.8	99.9
	50:50ZVI/VA	98.5	99.9	99.9	100	96.8	99.7	96.6
WZ	100VA	97.6	97.7	-688	-12.6	55.7	-22.0	94.5
	100ZVI	98.9	97.7	-18.1	4.9	66.5	-5.1	93.8
	50:50ZVI/VA	73.7	100.0	-495	0.3	82.1	-18.8	92.5

4.2 Column test results

Column tests were carried out for a period of 42 days, as discussed in Section 3.3. Treated water samples were drawn from the three ports positioned at 150 mm intervals along column height. After few days, it became impossible to continue running the 100ZVI column test as the reactive media rusted and solidfied to severely reduce hydraulic conductivity.

Figure 4 shows changes in concentrations of contaminants over distance along column height, for 50:50ZVI-VA substrate. It can be seen that contaminant removal from AMD solution follows simlar behaviour as observed in batch tests. Al, Fe, Zn were removed within the first port at 150 mm thickness. Also, Mg was removed from TDB but not from WZ, as already explained in Section 4.1.2. The behaviour exhibited by Mn is similar to that seen in batch test, being gradually removed from WZ while remaining unchanged in TDB.

4.3 Analytical studies

4.3.1 X-ray diffraction analyses

The crystalline structures existing at surface of the reactive media were examined by XRD analysis, conducted on ZVI and VA before and after their exposure to AMD. By comparing the mineralogical changes arising from interaction of these reactive media with AMD, the removal processes that occurred can be assessed. Figures 5 and 6 provide XRD patterns for ZVI and VA before and after their use to treat WZ or TDB. It can be seen in Figure 5 that non-reacted ZVI exhibited a single set of peaks at theta angles 35.6, 44.8 and 65.2^0, identified to be Iron, α-Fe. No other major peaks were observed, indicating high iron content in the ZVI, determined to be 80%Fe (Section 3.1). The reacted ZVI which had been used to treat AMD, developed new peaks, the major ones being at theta angles 43.3, 53.7, 57.2, 62.8^0 for samples WZ-ZVI and TDB-ZVI. It may be noted that the peak at 43.3^0 is a side-growth of the major peak at 44.8 in non-reacted ZVI. It is evident that intensity of the major peak observed in plain ZVI has reduced as a result of side-growth in WZ-100ZVI or TDB-100ZVI spectra, implying conversion of iron to a new reaction product(s). The rest of the peaks at 53.7, 57.2, 62.8^0 are completely new formations identified to be Hematite. While WZ-100ZVI and TDB-100ZVI showed mostly similar patterns, there was detectable presence of Goethite in the latter substrate taken from TDB treatment.

The complex mineralogy of non-reacted VA predominantly consisted of Diopside, Augite and Oxypyroxenes detected at theta angles of 26.8 to 28, 29.7 to 30.8, and 34.9 to 35.9^0. After the reaction of VA with AMD, these phases increased as visibly indicated by the stronger peaks of reacted WZ-100VA and TDB-100VA samples, relative to the non-reacted VA sample. The peak intensities of WZ-100VA were quite stronger compared to those for

TDB-100VA. More importantly, new phases consisting of Forsterite and Ferroans were formed as a result of VA reaction with AMD.

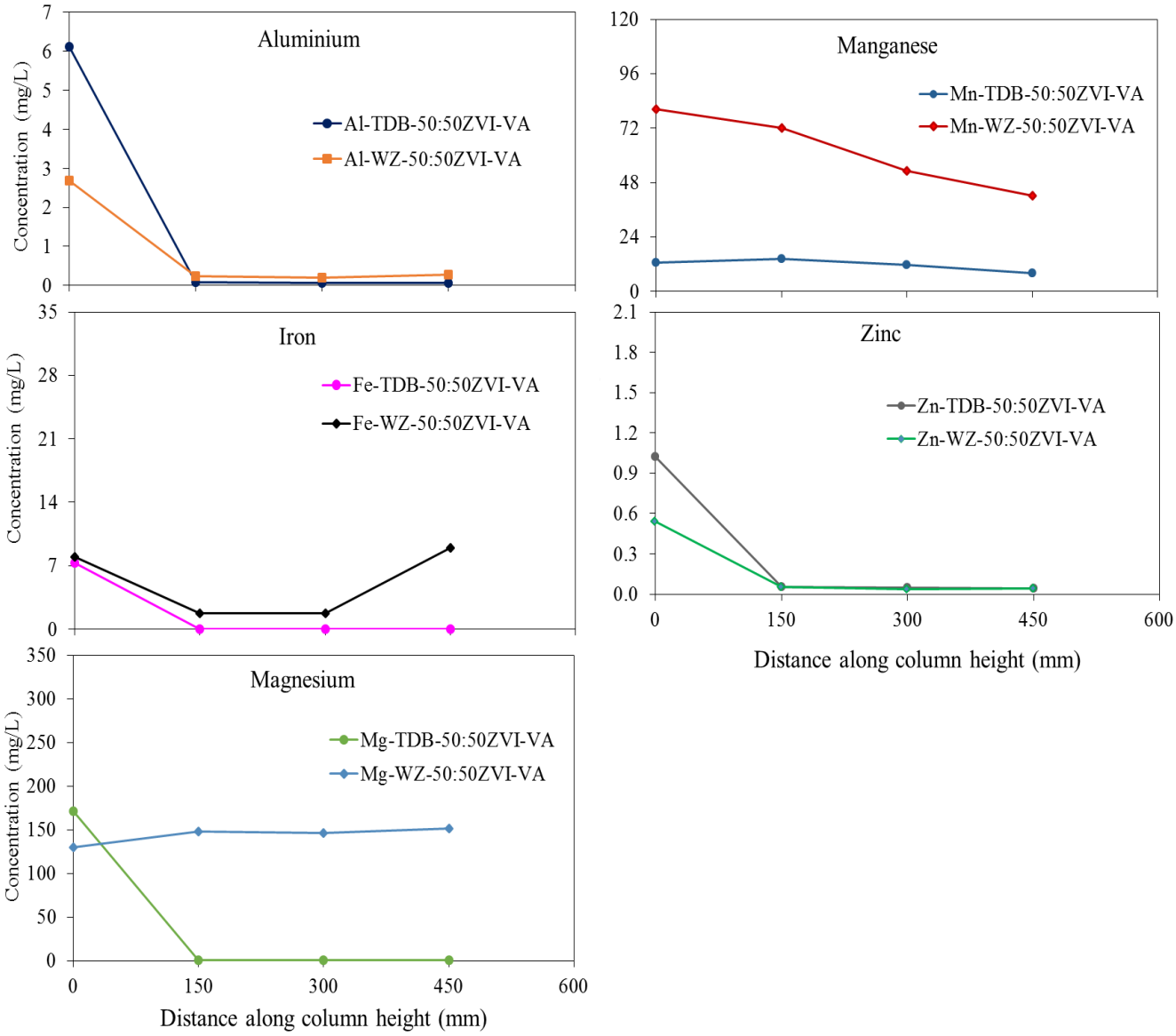

Figure 4. Changes in element concentrations for column tests of 50:50 ZVI/VA substrates, measured at 14 days

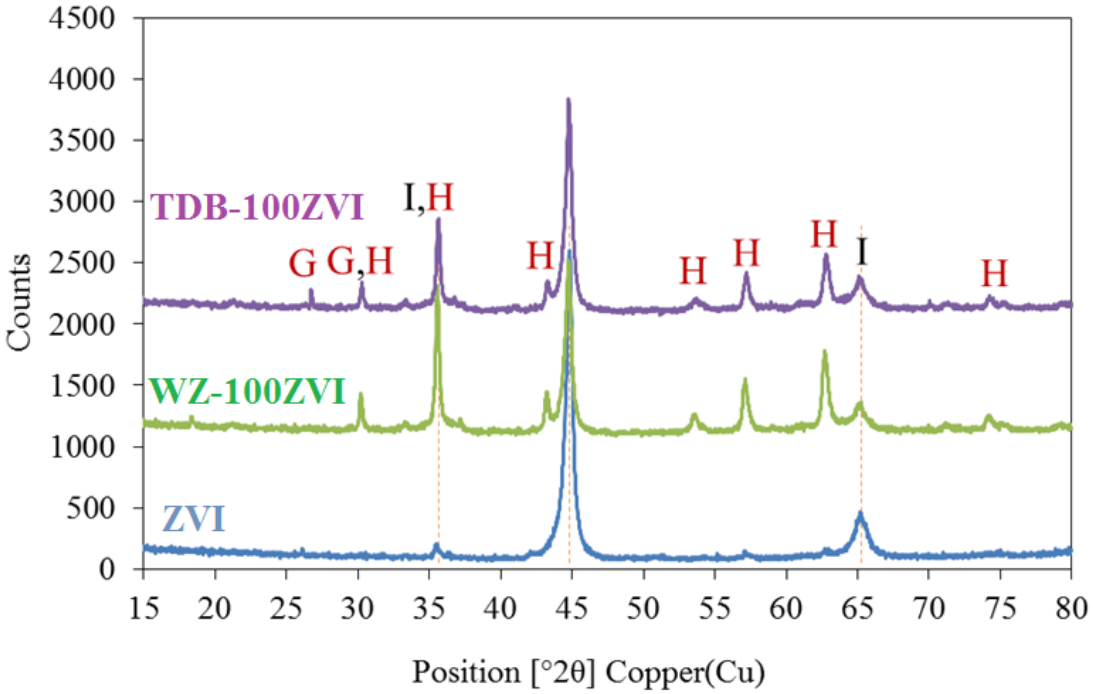

Figure 5. XRD patterns of zero-valent iron before and after exposure to acid mine drainage: I - Iron, Fe; H - Hematite, Fe_2O_3; G - Goethite, FeO(OH)

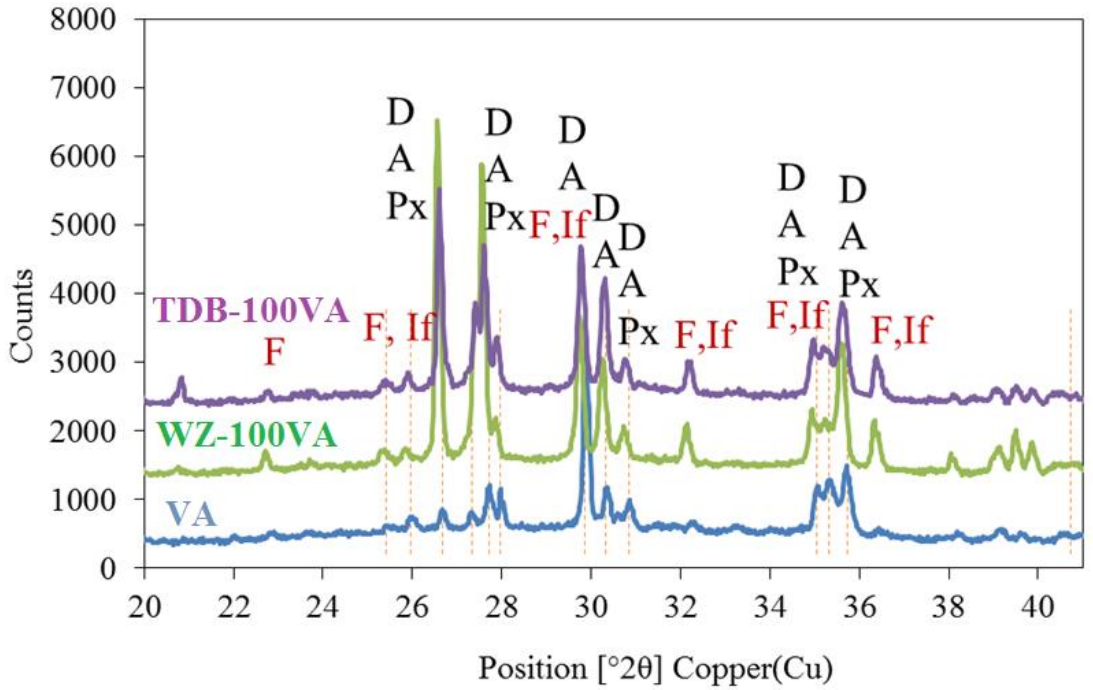

Figure 6. XRD patterns of volcanic ash before and after exposure to acid mine drainage: D – Diopside, A - Augite, Px - Orthopyroxene, F - Forsterite, If – Ferroan

4.3.2 Microscopic examination of zero-valent iron substrates

Solid residues of ZVI reactive media were prepared as explained in Section 3.5, and examined by SEM to evaluate morphology and spatial relationship among mineral precipitates at the surface of ZVI. SEM examination employs contrast in surface colour through its BSE mode. These contrasts are useful for differentiating the various types of elements, in which darker patches represent elements with higher atomic weight while lighter ones show groupings of elements with lower atomic weights. Figure 7a gives features of the ZVI before exposure to AMD i.e. unreacted ZVI. Elemental spot analysis showed the iron to be composed of 73% Fe, 24% O_2 and trace elements such as S, Cr, Mg and Mn. Figure 7a(i) shows characteristically angular and sharp edged, fractured ZVI particles. A close up of ZVI particle shown in Figure 7a(ii) indicates existing fissures characteristic of incomplete fracturing. Elemental mapping was done on a flat surface of ZVI shown in Figure 7a(iii). It can be seen in the EDS of Figure 7a(iv) that Fe and O_2 are the dominant elements in the ZVI (Luo et al., 2013).

There is evidence of change in the surface microstructure of ZVI after its exposure to TDB, showing a rougher surface texture seen in Figure 7b(i) and (ii). This change in ZVI texture can be attributed to formation of crystalline structures and precipitates arising from its reaction with AMD. Corrosion is seen to have occurred in Figures 7b(i) and (ii) showing the light coloured or brighter surface deposition confirmed by EDS to be iron oxides. The XRD analyses given in Section 4.3.1 identified this product to be Hematite.

Exhaustively reacted ZVI particles often show two main types of morphology, namely the acicular aggregates and cryptocrystalline clusters. Acicular aggregates are largely composed of rust minerals such as Goethite, Lepidocrocite or Metal Carbonates. Cryptocrystalline clusters usually contain poorly crystallized iron hydroxides. Inspection of Figures 7c(i) and

(ii) of the ZVI solid residues examined after exposure to WZ, reveals a change in surface texture exhibiting uneven surface and deposition of crystalline structures or precipitates at surface of the ZVI, as also observed in Figures 7b(i) and (ii) of TDB. In Figure 7c(ii), thin needle-like crystalline features can be seen. Figure 7c(iii) indicates these features to be some form of iron oxide or hydroxides. These structures are typical of Goethite (FeOOH) formation, a phase that was also detected through XRD analysis (Section 4.3.1).

4.3.3 Microscopic examination of zeolite substrates

Figure 8a gives features of naturally occurring VA zeolite prior to its use for AMD treatment in batch tests. Close inspection of the VA particles in Figure 8a(i) clearly shows the presence of large cavities at edges, which indicates a vesicular or honeycombed structure of its parent rocks. The close up shown in Figure 8a(ii) affirms this characteristic honeycombed structure of VA aggregates or rocks. Layered mapping of the VA particle surface given in Figure 8a(iii) shows a complex mixture of elements, seen in Figure 8a(iv). These are typical constituents of naturally occurring zeolites and are responsible for their effectiveness as natural filters. They possess a net negative charge, which is the driving force in removal of heavy metal contaminants through a cation exchange process.

Examination of VA that was exposed to TDB shows significant change in surface topography. In Figure 8b(i), the surface appears to be more angular and highly textured, in contrast to the plain surface seen in unreacted VA of Figure 8a(ii). These changes in texture are attributed to surface formation of crystalline structures through adsorption or ion exchange processes, causing metals to precipitate out of solution and attaching themselves to surface of the VA particles. Figure 8b(ii) also highlights the existence of two recurring unique features consisting of a light coloured siliceous phase and a darker iron-bearing phase, whose EDS signatures are shown in 8b(iii) and 8b(iv). XRD analyses (Section 4.3.1)

indicates the light siliceous phase to be possibly Forsterite while the darker iron-bearing phase is Ferroan. Figure 8c(i) shows changes in surface features of WZ-100VA samples, which are similar to those observed for TDB-100VA. Also, Ferroan and Forsterite phases are evident in Figure 8c(ii) and the associated EDS patterns of Figures 8c(iii) and (iv), respectively. Notable in Figure 8a(i) are hexagonal prismatic phenocrysts of olivine or pyroxene minerals, also observed in Ekolu et al. (2006). It may be recalled that presence of Orthopyroxenes was detected by XRD.

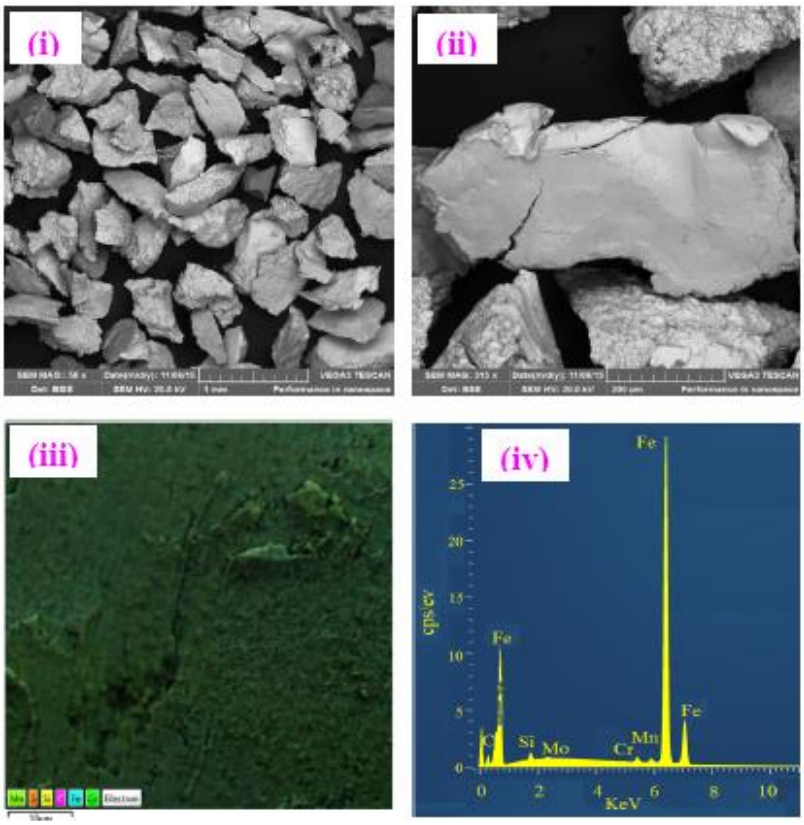

Figure 7a. SEM features of zero-valent iron before exposure to acid mine drainage

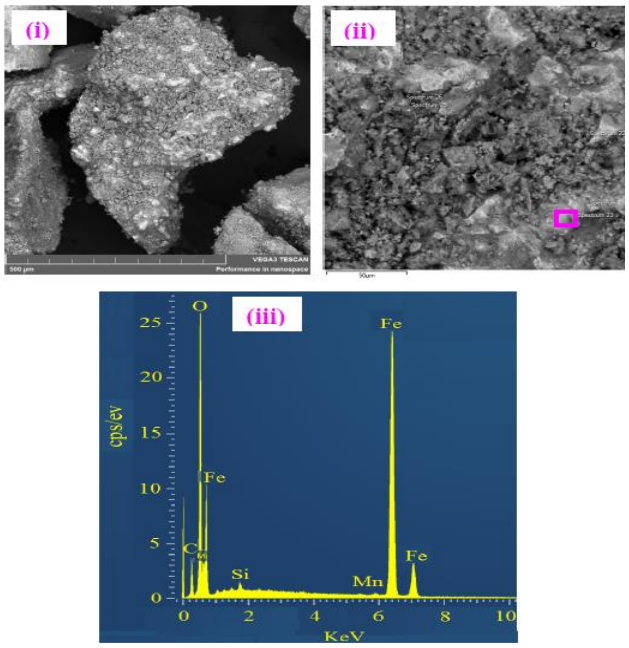

Figure 7b. SEM features of zero-valent iron for sample TDB-100ZVI after exposure to TDB: EDS was taken at spot marked by rectangle in (ii)

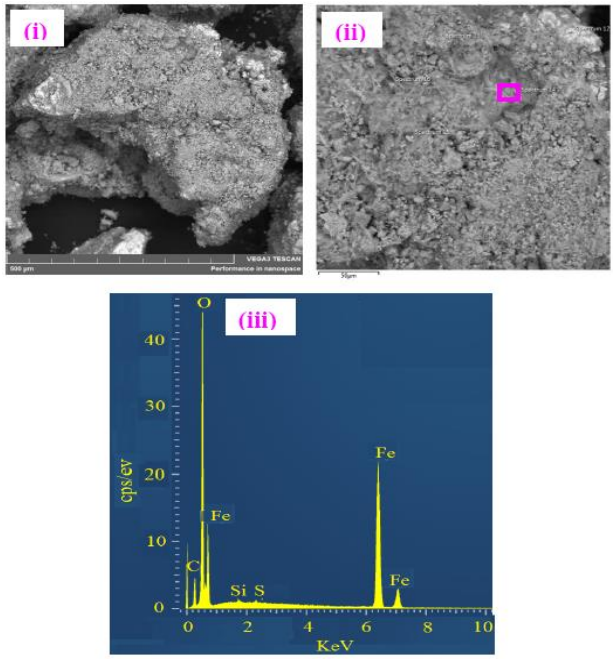

Figure 7c. SEM features of zero-valent iron for sample WZ-100ZVI after exposure WZ: EDS was taken at spot marked by rectangle in (ii)

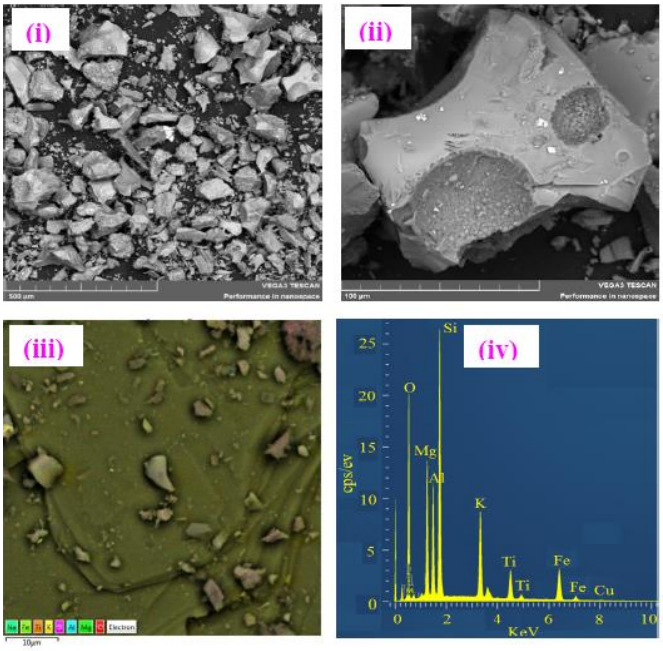

Figure 8a. SEM features of naturally occurring volcanic ash zeolite before exposure to acid mine drainage

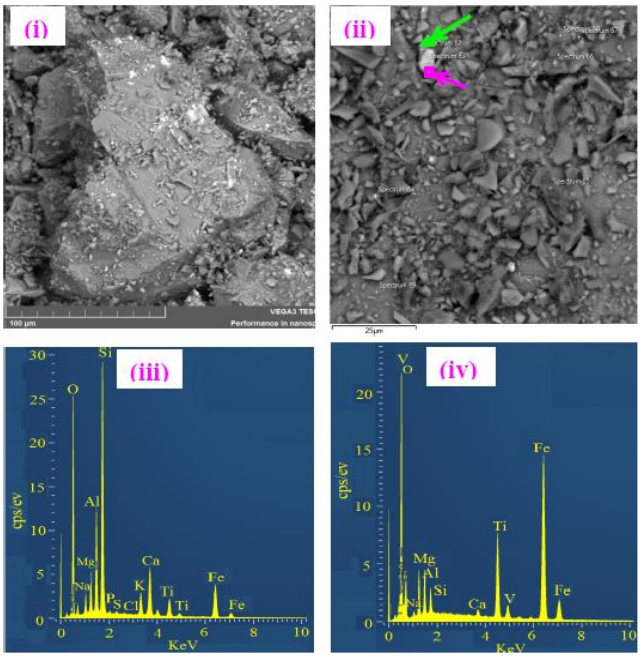

Figure 8b. SEM features of volcanic ash zeolite for sample TDB-VA after its exposure to TDB: EDS in (iii) is for upper (green) arrow in (ii); EDS in (iv) is for lower (pink) arrow in (ii)

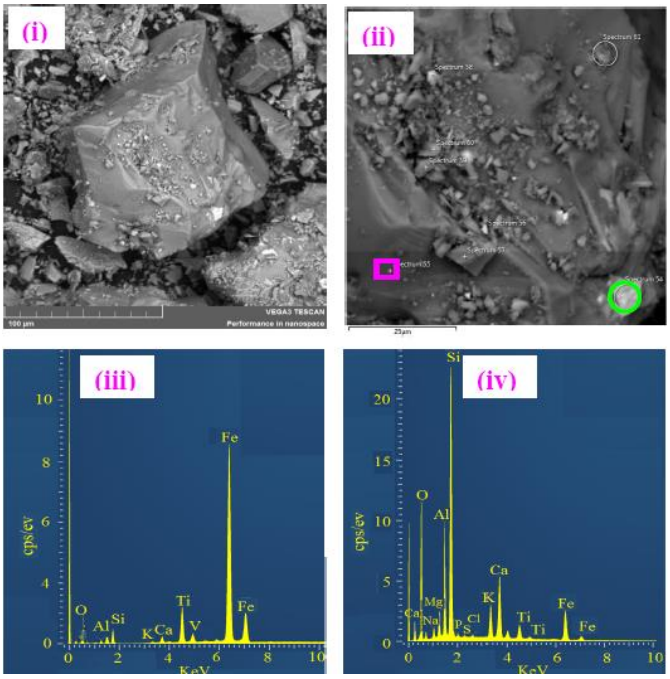

Figure 8c. SEM features of volcanic ash zeolite for sample WZ-VA after its exposure to WZ: EDS of (iii) was taken at a point marked by square in image (ii) identifying Ferroan; EDS of (iv) was taken at point marked by circle in image (ii) showing Forsterite

4.4 Contaminant removal processes

4.4.1 Removal mechanism(s) of zero-valent iron

When used as PRB reactive media, ZVI is known to be effective for contaminant removal from polluted aqueous systems through its redox reaction, which is an oxidation-reduction reaction involving the transfer of electrons from the reductant/reducing agent to the oxidant/oxidising agent. The iron acts as the reducing agent and oxidises to ferrous iron (Fe^{2+}) as per the Equation (1) (Simon and Meggyes, 2000; Suponik and Blanco, 2014). In an aerobic system, corrosion of the iron occurs as oxygen is the preferred oxidant. This causes ZVI to hydrolyse acidic water by forming hydroxide ions (Equation 2), which in turn increases the pH of water and consequently reduces the redox potential. Redox reactions

cause metals such as aluminium, zinc, nickel etc. to precipitate out of solution allowing them to be filtered out.

The ZVI itself is oxidised to ferrous hydroxide $Fe(OH)_2$ which may further oxidise to ferric hydroxide, $Fe(OH)_3$, as given by reaction Equations 2 and 3.

$$Fe^0(s) + O_2 + 2H_2O \rightarrow 2Fe^{2+} + 4OH^- \quad (1)$$

$$Fe^0(s) + 2H_2O \rightarrow Fe^{2+} + H_2 + 2OH^- \quad (2)$$

$$2Fe^{2+} + 2H_2O \rightarrow 2Fe^{3+} + H_2 + 2OH^- \quad (3)$$

With increase in pH to values between 5.0 to 12.0 under normal room temperature, geothite is easily forms from ferric hydroxide according to Equation (4). Also, hematite is formed at this same pH range up to values of 10, with optimum at pH = 7 to 8 (U. Schwertmann and E. Murad, 1983). Equations (5) and (6) show reactions leading to the formation of hematite and magnetite from ferrous hydroxide.

$$Fe^{3+} + 2H_2O \rightarrow FeOOH + 3H+ \quad (4)$$

$$2Fe^{2+} + 3H_2O \rightarrow Fe_2O_3 + 6H+ \quad (5)$$

$$3Fe^{2+} + 4H_2O \rightarrow Fe_3O_4 + 8H+ \quad (6)$$

In this study, effective chemical precipitation of heavy metals was expected to occur at pH range of 6 to 10, which was attained under ZVI treatment (Section 4.1.2, Figure 2) through the formation of their respective metal hydroxides (Aube, 2004; Seneviratne, 2007). XRD and SEM analyses (Sections 4.3.1 and 4.3.2) identified the formation of Hematite and Geothite in the reacted ZVI residues, which is consistent with the mechanism described in the foregoing. As mentioned earlier (Section 2.1), the precipitation of iron hydroxides and heavy

metals from solution as per Equations (1) to (6) leads to porosity loss and is responsible for reduction of hydraulic conductivity in reactive barrier systems (Wilkin and McNeil, 2003; Simon and Meggyes 2000).

4.4.2 Removal mechanism(s) of volcanic ash zeolite

It was observed in Section 4.1.1 (Figure 2) that both types of AMD, the WZ and TDB attained a maximum pH level of 5.5, when treated using only VA zeolite. Under this low pH level, most heavy metals are not expected to precipitate out of solution. However, the geochemical changes observed showed that the zeolite was effective in removal of heavy metals as discussed in Section 4.1.2. As such, it can be anticipated that the main removal mechanism for the zeolite was not pH-dependant but it probably involved cation exchange which is related to the crytal structures of the zeolite minerals. XRD patterns determined a mixture of Diopside and Augite to be the predominant minerals found in the natural VA zeolite. Diopside with unit cell formula $MgCaSi_2O_6$ was determined to be the main mineral phase while Augite ($(Ca,Na)(Mg,Fe,Al)(Al,Si)_2O_6$) was a minor mineral component. Also present where Orthopyroxenes whose silicate tetrahedra are typically connected by different elements forming variations such as Hypersthene ($(Mg,Fe)SiO_3$), Enstatite ($Mg_2Si_2O_6$), Ferrosilite ($Fe_2Si_2O_6$). The crystallographic structure of Diospide consists of chains of SiO_4 tetrahedra connected to each other at their corners by shared O_2 atoms which leaves a net ionic charge of -4. To balance this charge, these chains of SiO_4 tetrahedra are in turn connected to each other side by side by two octahedral sites (M1 and M2) which contain cations. M2 sites are larger than M1 sites, so large cations such as Ca and Na reside in M2 site, while small cations Fe and Mg cations occupy M1 sites. The bond between the SiO_4 tetrahedra and M1 sites is strong while that with M2 sites is generally weak. Accordingly, the

cations residing in M2 sites (Ca, Na) are more readily released into solution during cation exchange with ions in AMD solution.

In the present study, it is postulated that the various heavy metals (Na, Mg, Fe, Al etc) were adsorbed by zeolites, leading to growth in formation of Diopside and Augite, as observed by the intensification of XRD peaks. Also, some of the Ca in Diopside was readily released into AMD solution leading to the observed rise in pH. But since the VA zeolite contained a small constituent of only about 10% Ca, the pH increase is small, reaching a value of only 5.5. This release of Ca from Diopside transformed some of the mineral into a new phase, Fosterite (Mg_2SiO_4), which was identified by XRD. It is proposed that these cation exchange and adsorption mechanisms were responsible for the observed effectiveness of the natural zeolite in removing heavy metals from AMD.

5. Conclusions

In the foregone investigation, volcanic ash zeolite and zero-valent iron were evaluated as potential reactive media for use in permeable reactive barriers. Pollutant removal was studied and the associated mechanisms postulated. Since volcanic ash is an inexpensive natural zeolite, it would also provide a cost effective solution for remediation of acid mine drainage. It is found that while ZVI and VA are effective reactive media for treatment of acid mine drainage, however, their removal mechanisms are starkly different. The following findings are drawn:

(a) When treated using zero-valent iron, the TDB whose initial pH was 2.93 showed rapid rise in pH, achieving a higher peak pH = 8 to 8.5 compared to pH = 7 to 7.5 for WZ of initial pH = 2.46. In contrast, volcanic ash zeolite gave lower peak pH = 5.5 for both TDB and WZ but it showed faster rise in pH than zero-valent iron.

(b) Volcanic ash zeolite was found to be an effective reactive media for contaminant removal. In certain respects, the zeolite performed better than zero-valent iron. The reactive media comprising zero-iron valent, volcanic ash or their mixture were effective in near complete removal of Al, Fe, Zn while Mn could not be removed by any of the media. However, decrease in Mn was observed, which is thought to be a result of co-precipitation with Fe. Mg was also not removed by the media systems except in TDB where delayed removal occurred as pH approached closer to 9, a value required for the metal removal.

(c) Column tests that were conducted using a substrate comprising a mixture of 50% zero-valent iron and 50% volcanic ash zeolite, gave results that were consistent with observations made in batch tests. The mixture was found to effectively remove major inorganic contaminants from both types of acid mine drainage, except Mn and Mg.

(d) It was found that zero-valent iron formed new phases of Hematite and Goethite upon reacting with acid mine drainage, while reacted volcanic ash zeolite formed Forsterite and Ferroan as the new phases.

(e) Chemical precipitation was found to be the most likely mechanism of contaminant removal by ZVI, while zeolite was found to effectively remove heavy metals through the mechanisms of adsorption and cation exchange.

Acknowledgements

The study presented in this paper was supported by the National Research Foundation (NRF) of South Africa, IPRR Grant No. 96800. The authors are grateful for the support given by NRF.

References

Abdel Rahmana R.O., Abdel Moamena O.A., Hanafyb M., Abdel Monemb N.M. (2012), Preliminary investigation of zinc transport through zeolite-X barrier: linear isotherm assumption, Chemical Engineering Journal 185– 18661– 70

Abdel Salam O.E., Reiad N.A., El Shafei M.M. (2011), A study of the removal characteristics of heavy metals from wastewater by low-cost adsorbents, Journal of Advanced Research 2, 297–303.

Aube B. (2004), The science of treating acid mine drainage and smelter effluents, 361 Aumais, Ste-Anne-de-Bellevue, Quebec, Canada, 23p. www.enviraube.com (accessed 18 June 2017).

Bartzas G., Komnitsas K. and Paspaliaris I. (2006), Laboratory evaluation of Fe 0 barriers to treat acidic leachates. Minerals Engineering, 19(5), 505-514.

Basaldella E.I, Vázquez P.G, Iucolano F., Caputo D. (2007),Chromium removal from water using LTA zeolites: Effect of pH, Journal of Colloid and Interface Science 313 574–578.

Bilardi (2011), Short and long-term behaviour of Fe^0 AND Fe^0 /pumice granular mixtures to be used in PRB for groundwater remediation, Mediterranea University of Reggio Calabria, DICEAM, Dissertation, 153p.

Bosco S.M.D, Jimenez R.S, Carvalho W.A. (2005), Removal of toxic metals from wastewater by Brazilian natural scolecite, Journal of Colloid and Interface Science, 281, Issue 2, 15 January, 424-431.

Calabrò P.S, Moraci N., Suraci P. (2012), Estimate of the optimum weight ratio in Zero-Valent Iron/Pumice granular mixtures used in permeable reactive barriers for the remediation of nickel contaminated groundwater,Journal of Hazardous Materials 207–208 111–116.

Cundy A.B., Hopkinson L. and Whitby R.L. (2008), Use of iron-based technologies in contaminated land and groundwater remediation: A review. Science of the Total Environment, 400(1), 42-51.

Cyrus J.S. and Reddy G. (2011), Sorption and desorption of ammonium by zeolite: Batch and column studies. Journal of Environmental Science and Health Part A, 46(4), 408-414.

Day S.R., O'hannesin S.F. and Marsden L. (1999), Geotechnical techniques for the construction of reactive barriers. Journal of hazardous materials, 67(3), 285-297.

Delkash M., Bakhshayesh B.E. and Kazemian H. (2015), Using zeolitic adsorbents to cleanup special wastewater streams: A review. Microporous and Mesoporous Materials, 214, 224-241.

Díaz I. (2017), Environmental uses of zeolites in Ethiopia, Catalysis Today, 285 29–38.

Ekolu S.O, Thomas M.D.A, and Hooton R.D (2006), Studies on Ugandan volcanic ash and tuff, Proc. 1st Intl. Conf. on Advances in Engineering and Technology, Entebbe, Uganda, July, 75-83.

Ekolu S.O., Azene F.Z., Diop S. (2014), A concrete reactive barrier for acid mine drainage treatment, Proc. Inst. Civil Eng. Water Manag. 167 373–380.

Ekolu S.O., Diop S., Azene F.Z. (2016), Properties of pervious concrete for hydrological applications, Concrete Beton, J. Concr. Soc. S. Africa, March 2016, 18–24.

Erdem E., Karapinar N. and Donat R. (2004), The removal of heavy metal cations by natural zeolites. Journal of colloid and interface science, 280(2), 309-314.

Fu F. and Wang Q. (2011), Removal of heavy metal ions from wastewaters: A review. Journal of environmental management, 92(3), 407-418.

Fuhrmann M., Aloysius D., Zhou H. (1995), Permeable, subsurface sorbent barrier FOR 9°Sr: laboratory studies of natural and synthetic materials, Waste Management, 15 (7), 485-493.

Gavaskar A. (1999), Design and construction techniques for permeable reactive barriers. Journal of hazardous materials, 68(1–2), 41-71.

Gavaskar, A., B. Sass, N. Gupta, J. Hicks, S. Yoon, T. Fox, and J. Sminchak. 1998. Performance evaluation of a pilot-scale permeable reactive barrier at former Naval Air Station Moffett Field, Mountain View, California. Final report prepared by Battelle, Columbus, Ohio for Naval Facilities, Engineering Service Center, Port Hueneme, CA. Project Sponsored by ESTCP, 191p.

Harrison R.M., 2007. Principles of Environmental Chemistry. 1st Ed. Cambridge: Royal Society of Chemistry, ISBN: 9781615833696 1615833692, 363p.

Hashim M.A., Mukhopadhyay S., Sahu J.N. and Sengupta B. (2011), Remediation technologies for heavy metal contaminated groundwater. Journal of Environmental Management, 92(10), 2355-2388.

Inglezakis V.J. (2005), The concept of “capacity” in zeolite ion-exchange systems, Journal of Colloid and Interface Science 281, 68–79.

Itskos G., Koutsianos A., Koukouzas N., Vasilatos C. (2015), Zeolite development from fly ash and utilization in lignite mine-water treatment, International Journal of Mineral Processing 139 43–50.

Jeen S-W, Gillham R.W, Przepiora A. (2011), Predictions of long-term performance of granular iron permeable reactive barriers: Field-scale evaluation, Journal of Contaminant Hydrology, 123, 50–64.

Johnson T., Tratnyek P.G., Scherer M. and Matheson L.J. (2003), Permeable reactive barriers of iron and other zero-valent metals. Environmental Science and Pollution Control Series, 371-422.

Johnson T.L., Scherer M.M. and TRatnyek, P.G. (1996), Kinetics of halogenated organic compound degradation by iron metal. Environmental Science & technology, 30(8), 2634-2640.

Klimkova S., Cernik M., Lacinova L., Filip J., Jancik D. and Zboril R. (2011), Zero-valent iron nanoparticles in treatment of acid mine water from in situ uranium leaching. Chemosphere, 82(8), 1178-1184.

Komnitsas K, Bartzas G., Fytas K., Paspaliaris I. (2009), Long-term efficiency and kinetic evaluation of ZVI barriers during clean-up of copper containing solutions, Minerals Engineering, 20 (13), 1200-1209.

Li C., Zhong H., Wang S., Xue J. and Zhang Z. (2015), A novel conversion process for waste residue: Synthesis of zeolite from electrolytic manganese residue and its application to the removal of heavy metals. Colloids and Surfaces A: Physicochemical and Engineering Aspects, 470, 258-267.

Lien H.L. and Wilkin R.T. (2005), High-level arsenite removal from groundwater by zero-valent iron. Chemosphere, 59(3), 377-386.

Luo P., Bailey E.H, Moone S.J. (2013), Quantification of changes in zero valent iron morphology using X-ray computed tomography, Journal of Environmental Sciences, 25(11), 2344–2351.

Mackenzie P.D., Horney D.P. and Sivavec T.M. (1999), Mineral precipitation and porosity losses in granular iron columns. Journal of Hazardous Materials, 68(1), 1-17.

Moraci N, Calabrò P.S. (2010), Heavy metals removal and hydraulic performance in zero-valent iron/pumice permeable reactive barriers, Journal of Environmental Management, 91 2336e234.

Morrison S.J, Naftz D.L, Davis J.A, Fuller C.C. (2003), Chapter 1 - Introduction to groundwater remediation of metals, radionuclides, and nutrients with permeable reactive barriers, Handbook of Groundwater Remediation using Permeable Reactive Barriers, 1-15. http://0-www.sciencedirect.com/

Motsi T., Rowson N.A. and Simmons M.J.H. (2009), Adsorption of heavy metals from acid mine drainage by natural zeolite. International Journal of Mineral Processing, 92(1–2), 42-48.

Mulligan C.N., Yong R.N. and Gibbs B.F. (2001). Remediation technologies for metal-contaminated soils and groundwater: an evaluation. Engineering Geology, 60 (1–4), 193-207.

Mumford K.A, Rayner J.L, Snape I, Stark S.C, Stevens G.W, Gore D.B (2013), Design, installation and preliminary testing of a permeable reactive barrier for diesel fuel remediation at Casey Station, Antarctica, Cold Regions Science and Technology 96 96–107.

Mumford K.A, Rayner J.L, Snape I, Stevens G.W, (2014), Hydraulic performance of a permeable reactive barrier at Casey Station, Antarctica, Chemosphere, 117, 223–231.

Nekhunguni P.M, Tavengwa N.T, Tutu H. (2017), Investigation of As(V) removal from acid mine drainage by iron (hydr)oxide modified zeolite, Journal of Environmental Management 197 550e558.

Obiri-Nyarko F., Grajales-Mesa S.J, Malina G. (2014), An overview of permeable reactive barriers for in situ sustainable groundwater remediation, Chemosphere, 111, 243-259.

PItcher S.K., Slade R.C.T. and Ward N.I. (2004), Heavy metal removal from motorway stormwater using zeolites. Science of the Total Environment, 334–335, 161-166.

Querol X., Alastuey A., Moreno N., Alvarez-Ayuso E., Garcia-Sanchez A, Cama J, Ayora C., Simon M. (2006), Immobilization of heavy metals in polluted soils by the addition of zeolitic material synthesized from coal fly ash, Chemosphere, 62 171–180.

Ríos C.A, Williams C.D, Roberts C.L. (2008), Removal of heavy metals from acid mine drainage (AMD) using coal fly ash, natural clinker and synthetic zeolites, Journal of Hazardous Materials, Aug 15;156 (1-3):23-35. doi: 10.1016/j.jhazmat.2007.11.123. Epub 2007 Dec 14.

Ruhl A.S, Jekel M. (2012), Impacts of Fe(0) grain sizes and grain size distributions in permeable reactive barriers, Chemical Engineering Journal 213 245–250.

Schwertmann U. and Murad E. (1983), Effect of pH on the formation of goethite and hematite from ferrihydrate, Clay and Clay Minerals, 31 (4), 277-284.

Seneviratne M. (2007) A Practical approach to water conservation for commercial and industrial facilities, Queensland Water Commission, Elsevier Ltd, ISBN 978-1-85-617489-3, 372p.

Shabalala A.N, Ekolu S.O, Diop S., Solomon F. (2017), Pervious concrete reactive barrier for removal of heavy metals from acid mine drainage − column study, Journal of Hazardous Materials, 323, Part B, 5 February, 641-653

Simon F. and Meggyes T. (2000), Removal of organic and inorganic pollutants from groundwater using permeable reactive barriers, Land Contamination & Reclamation, 8(2), 103-116.

Suponik T. and Blanco M. (2014), Removal of heavy metals from groundwater affected by acid mine drainage, physicochemical problems of mineral processing, 50 (1), 359-371.

Thiruvenkatachari R., Vigneswaran S. and Naidu R. (2008), Permeable reactive barrier for groundwater remediation. Journal of Industrial and Engineering Chemistry, 14, 145–156.

Toscano G., Caristi C, Cimino G. (2008), Sorption of heavy metal from aqueous solution by volcanic ash, C. R. Chimie 11 765e771.

Waite T.D, Desmier R., Melville M., Macdonald B. (2003), Chapter 3 - Preliminary investigation into the suitability of permeable reactive barriers for the treatment of acid sulfate soils discharge, Handbook of Groundwater Remediation using Permeable Reactive Barriers, 2003, 67-104.

Wajima T. (2013), Ion exchange properties of Japanese natural zeolites in seawater, Analytical Sciences, The Japan Society for Analytical Chemistry, January, Vol. 29, 139-144.

Wan C., Ding S., Zhang C., Tan X.b, Zou W., Liu X., Yang X (2017), Simultaneous recovery of nitrogen and phosphorus from sludge fermentation liquid by zeolite adsorption: Mechanism and application, Separation and Purification Technology 180, 1–12.

Weber A, Ruhl A.S, Amos R.T (2013), Investigating dominant processes in ZVI permeable reactive barriers using reactive transport modelling , Journal of Contaminant Hydrology, 151, 68–82.

Wilkin R.T. and McNeil M.S. (2003), Laboratory evaluation of zero-valent iron to treat water impacted by acid mine drainage. Chemosphere, 53(7), 715-725.

Xenidis A., Moirou A. and Paspaliaris I. (2002), Reactive materials and attenuation processes for permeable reactive barriers. Mineral Wealth, 123(1), 35-48.